Volume 1 | Number 1 | Jan 2013 | Pages 1–100

Organic & Biomolecular Chemistry

www.rsc.org/obc

ROYAL SOCIETY OF CHEMISTRY

This is an *Accepted Manuscript*, which has been through the Royal Society of Chemistry peer review process and has been accepted for publication.

Accepted Manuscripts are published online shortly after acceptance, before technical editing, formatting and proof reading. Using this free service, authors can make their results available to the community, in citable form, before we publish the edited article. We will replace this *Accepted Manuscript* with the edited and formatted *Advance Article* as soon as it is available.

You can find more information about *Accepted Manuscripts* in the **Information for Authors**.

Please note that technical editing may introduce minor changes to the text and/or graphics, which may alter content. The journal's standard **Terms & Conditions** and the **Ethical guidelines** still apply. In no event shall the Royal Society of Chemistry be held responsible for any errors or omissions in this *Accepted Manuscript* or any consequences arising from the use of any information it contains.

ROYAL SOCIETY OF CHEMISTRY

Journal Name

ARTICLE

The synthesis of a pyridine-*N*-oxide isophthalamide rotaxane utilizing supplementary amide hydrogen bond interactions

Nicholas H. Evans,* Charles E. Gell and Michael J. G. Peach

The synthesis of a pyridine-*N*-oxide containing rotaxane, not requiring an additional ionic template, has been achieved in 32% yield. Successful rotaxane formation is dependent upon the structure of the isophthalamide macrocycle used, an observation which has been rationalised by a combination of NMR spectroscopy, X-ray crystallography and computational modelling.

Introduction

Rotaxanes,[1] interlocked molecules consisting of macrocyclic ring(s) trapped on a stoppered axle, are increasingly being used in a range of functional applications.[2, 3] Underpinning this work has been the development of template methodologies to overcome the otherwise entropically unfavourable association of molecular components required for the preparation of a rotaxane. Popular choices of templates and templating interactions that have been used to prepare rotaxanes include: metal cations,[4] anions,[5] π-π stacking[6] and hydrogen bonding.[7] While a significant number of template methodologies for the production of rotaxanes have now been reported, the establishment of further versatile synthetic pathways has the potential to aid the supramolecular chemistry community in the preparation of new, functionally useful rotaxanes.

The hydrogen bond templated threading of simple 3, 5-bisamides of pyridine-*N*-oxides through isophthalamide macrocycles to form pseudo-rotaxanes has been reported by Jiang and co-workers (Figure 1).[8] Considering the synthetic ease in the generation of 3, 5-bisamides of pyridine-*N*-oxides (including the possibility of installing different substituents on each amide) and isophthalamide macrocycles, such a self-assembled array looks attractive to be incorporated into the synthesis of a fully interlocked rotaxane. However, to date there is a lack of rotaxane syntheses using the system as described by Jiang *et al*. Beer and co-workers have reported on a number of rotaxanes containing 3, 5-bisamide pyridine-*N*-oxide motifs, but appreciable yields of formation are only observed in the presence of an additional cationic[9,10,11] or anionic[12] template. To the best of our knowledge, only one

synthesis of a fully interlocked rotaxane using the simple self-assembly motif as described by Jiang *et al* without recourse to further ionic templation has been disclosed, but the rotaxane was only isolated in the somewhat modest yield of 15%.[13]
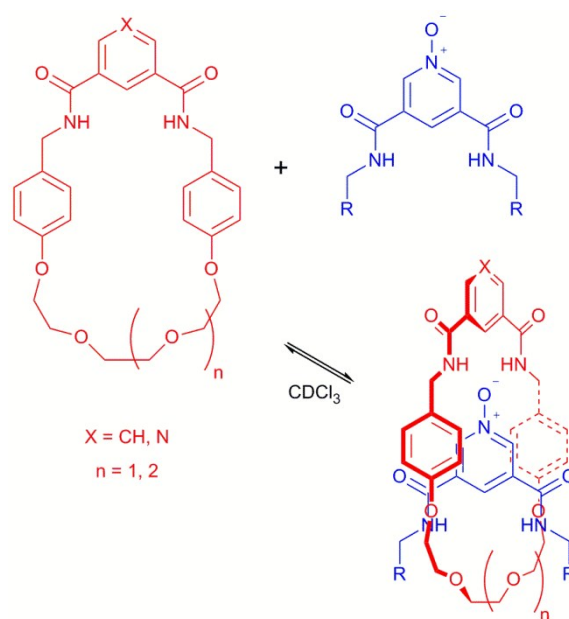

Figure 1: Formation of a hydrogen bond templated pseudo-rotaxane consisting of an isophthalamide macrocycle and unstoppered pyridine-*N*-oxide axle, as reported by Jiang and co-workers, ref. 8.

Herein we report the synthesis of a fully interlocked rotaxane in a 32% yield, by use of the CuAAC click reaction to stopper a 3, 5-bisamide pyridine-*N*-oxide axle threaded through a polyether containing isophthalamide macrocycle, without the use of additional templation from either a cation or anion to support the self-assembly of the pseudo-rotaxane intermediate. An attempted synthesis with a second isophthalamide macrocycle, containing a benzene ring in place of the polyether chain, yielded no rotaxane. Solution NMR spectroscopy, solid state crystallography and computational

Department of Chemistry, Lancaster University, Lancaster, LA1 4YB, UK.
E-mail: n.h.evans@lancaster.ac.uk

Organic & Biomolecular Chemistry Accepted Manuscript

ARTICLE

Journal Name

modelling have been used to explain the different synthetic outcomes in these two systems.

Results and discussion

Macrocycle synthesis

The two macrocycles, **1** and **2**, investigated in this study are depicted in Figure 1. Each contains an isophthalamide motif that may hydrogen bond to a suitable hydrogen bond acceptor, such as the oxygen atom of a pyridine-*N*-oxide. With a view to preparing more sophisticated rotaxanes in the future, there is the possibility of incorporating functionality on the isophthalamide ring of both macrocycles by use of 5-substituted isophthalamides. In addition, the inclusion of an additional aromatic ring in the structure of **2** allows for similar opportunities at the other end of this macrocycle.
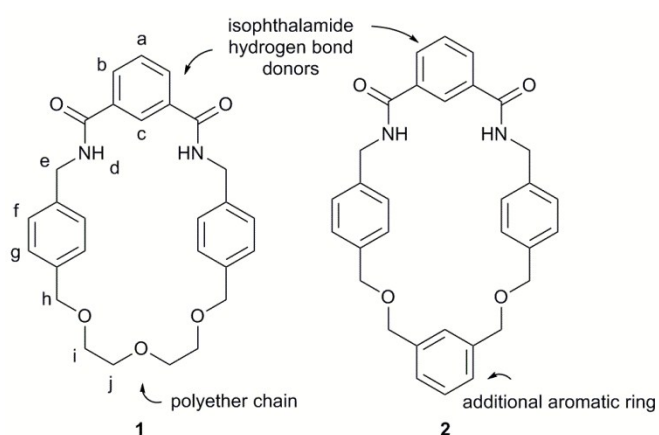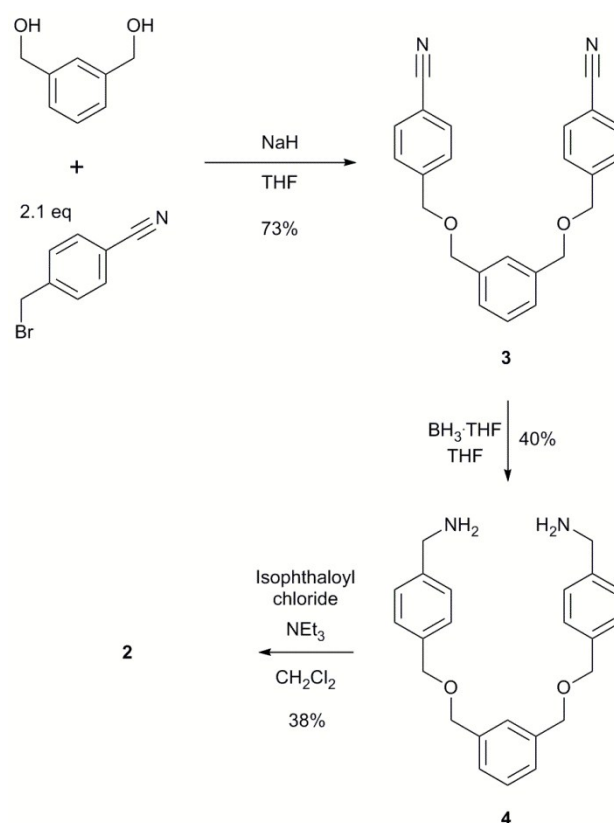

Figure 2: Structures of macrocycles **1** and **2**.

The synthesis of macrocycle **1** has been reported previously.[14] Macrocycle **2** was prepared by an analogous synthetic route (Scheme 1). Alkylation of (benzene-1,3-diyl)dimethanol with 2.1 equivalents of 4-(bromomethyl)benzonitrile afforded compound **3** in 73% yield. Bis-nitrile **3** was then reduced to bis-amine **4** using borane-THF in an isolated 40% yield. Bis-amine **4** was then reacted, under high dilution conditions, with one equivalent of isophthaloyl chloride in the presence of excess triethylamine, in dichloromethane. After aqueous work-up and silica gel chromatography, macrocycle **2** was isolated in 38% yield. In addition to characterisation by NMR and IR spectroscopy and mass spectrometry, crystals of **2** suitable for single crystal X-ray diffraction were grown by slow evaporation of a chloroform sample confirming the macrocyclic nature of **2** (see ESI†).
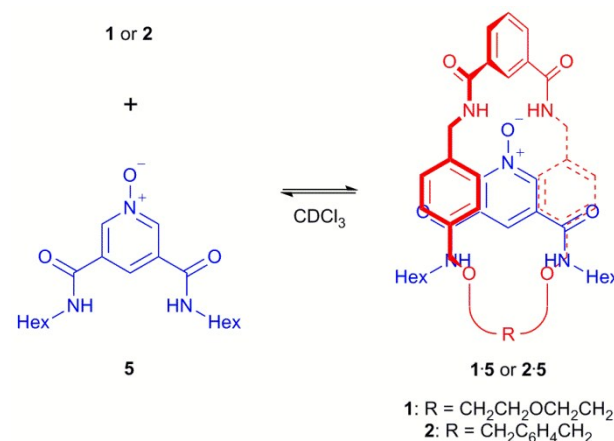
Experimental pseudo-rotaxane investigations

With **1** and **2** in hand, ^{1}H NMR spectroscopy was used to investigate the ability of a 3, 5-bisamide pyridine-*N*-oxide motif to thread through the macrocycles. Equimolar amounts of macrocycle (**1** or **2**) and unstoppered pyridine-*N*-oxide thread **5**[11] were dissolved in CDCl$_3$, a relatively uncompetitive solvent

with respect to hydrogen bonding, and ^{1}H NMR spectra recorded (Scheme 2).

Scheme 1: Synthesis of macrocycle **2**.

Scheme 2: Attempted formation of pseudo-rotaxanes **1·5** and **2·5**.

Upon the addition of **5** to macrocycle **1**, the aromatic resonances *f* and *g* split and moved upfield in the ^{1}H NMR spectrum (Figure 3). This is consistent with intercalation of the pyridine-*N*-oxide ring of **5** between the aromatic rings of macrocycle **1**, confirming that pseudo-rotaxane **1·5** has formed.[16] In contrast, only a very modest movement of the equivalent aromatic resonances of macrocycle **2** were observed in the ^{1}H NMR spectrum upon addition of **5** (see ESI†), indicating that little (if any) pseudo-rotaxane formation occurred between **2** and **5**.
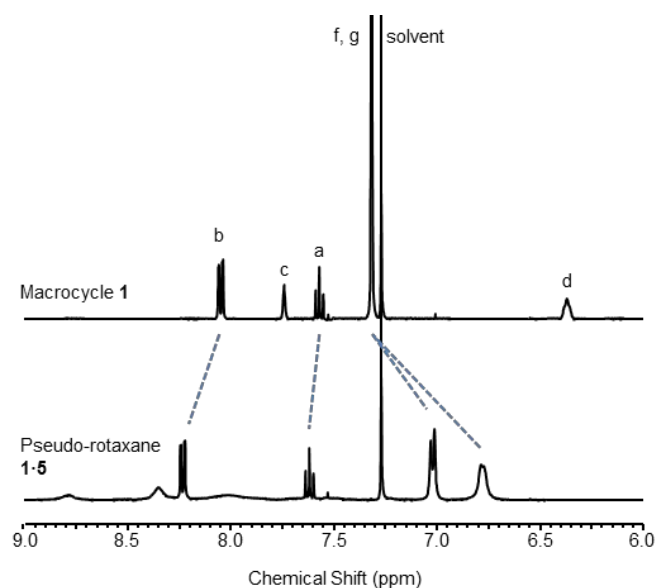
Figure 3: Partial ^{1}H NMR spectra of macrocycle **1** and pseudo-rotaxane **1·5** (CDCl$_3$, 5 mM, 400 MHz, 298 K). For atom labels see Figure 2.

Single crystals suitable for single crystal X-ray diffraction were grown by the slow diffusion of isopropyl ether into the deuterated chloroform solution containing **1** and **5**. The solved structure revealed the interpenetrated structure of pseudo-rotaxane **1·5** (Figure 4).
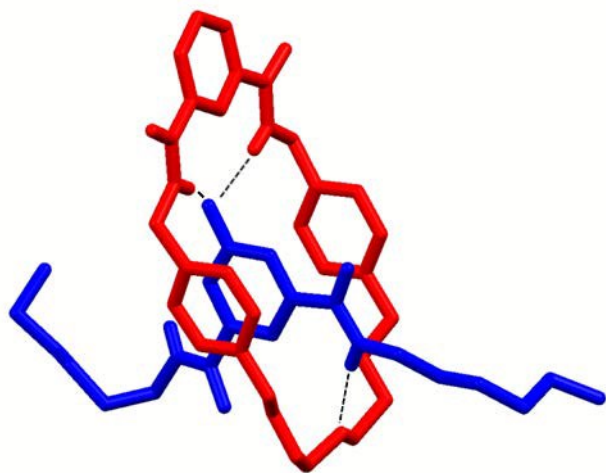

Figure 4: X-ray structure of pseudo-rotaxane **1·5**. Hydrogen atoms (except N-Hs) and disorder in one of the hexyl chains are omitted for clarity.

As expected there are hydrogen bonds between the isophthalamide N-Hs to the oxygen atom of the pyridine-*N*-oxide (N-H···O distances: 2.151 Å and 2.221 Å). In addition, there is a hydrogen bond interaction between the *syn* pyridine-*N*-oxide amide N-H to the central polyether oxygen (N-H···O distance: 2.129 Å). Based on this crystal structure, we tentatively attributed the failure of macrocycle **2** and thread **5** to form a pseudo-rotaxane in solution to the lack of an appropriately positioned atom in macrocycle **2** to form an equivalent hydrogen bond with the amide N-H of the pyridine-*N*-oxide bis-amide thread **5**.

Computational study of pseudo-rotaxanes

To provide further insight into the experimental results of the pseudo-rotaxane studies, density-functional theory (DFT) calculations were undertaken on macrocycles **1** and **2**, thread **5** and the possible pseudo-rotaxanes **1·5** and **2·5**.[17] The calculations were performed using the Gaussian 09 program,[18] using the B3LYP functional[19] together with the 6-31G* basis set for all atoms. Solvent effects (CHCl$_3$) were modelled using the standard polarizable continuum model, with the default Gaussian 09 parameters for the solvent and cavity. Dispersion interactions were also approximated via Grimme's D3 dispersion correction.[20] In each case, an optimised structure was obtained; vibrational frequencies were computed to ensure each structure was in fact a minimum on the potential energy surface, and to quantify the zero-point energy corrections.

The isolated macrocycles were modelled first. In the case of macrocycle **1**, the minimum energy structure in solution (see Figure 5) was found to closely resemble that of the previously reported crystal structure,[14] and the obtained structure would seem to favour the possibility of threading due to the potential for intermolecular hydrogen bonding and π–π stacking interactions. However, in the case of macrocycle **2**, there were two distinct structures found; the first, based on the crystal structure, is the more stable, but the resultant structure (see Figure 5) would not favour appropriate hydrogen bonding or π–π stacking interactions when threaded. The second, higher energy conformation (see ESI†), more closely resembles the minimized structure of macrocycle **1**.
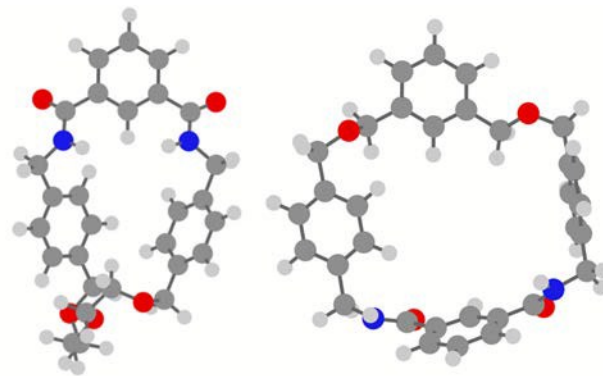

Figure 5: Minimum energy structures of macrocycles **1** (left) and **2** (right); each closely resembles the observed crystal structure of the respective macrocycle.

A number of conformations of thread **5** were then considered. These included *syn-syn*, *syn-anti* and *anti-anti* conformations, additionally allowing for possible rearrangement in the terminal alkyl chains. The lowest energy conformation was found to be the *syn-anti* conformation, and the highest energy the *anti-anti* conformation, with the difference in energies between the most and least stable being less than 10 kJ mol^{-1}.

After these initial calculations, the structural and energetic properties of the pseudo-rotaxanes **1·5** and **2·5** were considered. Three conformations (*syn-syn*, *syn-anti* and *anti-anti*) of thread **5** were examined, to determine which

conformation was associated with the most stable pseudo-rotaxane; i.e., which of the three possible conformations of the thread is able to most strongly interact with the macrocycle unit.

For the geometry optimisations of pseudo-rotaxane **1·5**, two sets of starting points were considered, to minimise bias and to maximise the chance of finding the global minimum on the potential energy surface. Firstly, structures based around the observed crystal structure of the pseudo-rotaxane, and secondly 'free-hand' structures drawn to maximise intermolecular interactions were considered. The structures based on the free-hand starting geometries were in each case found to give a final structure lower in energy (i.e., more stable) than the corresponding crystal-structure based starting points. However, the structures are qualitatively similar in all cases. Indeed, irrespective of the starting geometries, the stability of pseudo-rotaxane **1·5** was found to be greatest for the *syn-syn* thread conformation (depicted in Figure 6), and least for the *anti-anti* conformation. A relatively small difference in stability between the *syn-syn* and *syn-anti* conformation was observed. Examination of the crystal structure data suggests that for pseudo-rotaxane **1·5**, the *syn-anti* conformation is preferred; we attribute this preference to crystal packing effects in the solid state.

There is good correlation between the O-H$_c$ distance and the stability of the conformation (the shorter the hydrogen bond distance, the more stable the conformation) for pseudo-rotaxane **1·5** (Table 1). There are a range of average ring-ring distances in the range of 3.65 to 3.93 Å (the thread does not sit in the middle of the macrocycle), but these vary only slightly between the conformations, suggesting that the $\pi-\pi$ interactions are similar irrespective of the conformation.

Table 1: Inter-component hydrogen bond distances between H$_c$ of macrocycles **1** and **2** and pyridine-*N*-oxide O of thread **5** in simulated pseudo-rotaxanes **1·5** and **2·5**.[a]

	1	**2**
syn-syn	2.036	2.046
syn-anti	2.065	2.068
anti-anti	2.337	2.311

[a] Distances in Å

For the free-hand based starting geometries, the stability of pseudo-rotaxane **1·5** relative to individual **1** and **5** were then considered. To evaluate these quantities, the energy of the most stable found structures of the macrocycle and thread (irrespective of conformation) were subtracted from the energy of the pseudo-rotaxane with the thread in each of the three conformations. Here, the *syn-syn* conformation has the lowest energy. Relative to that lowest energy conformation, the *syn-anti* and *anti-anti* conformation was found to be 11 kJ mol^{-1} and 32 kJ mol^{-1} higher in energy respectively. Regardless of the choice of conformation of the thread, the pseudo-rotaxane was found to be stable relative to the individual macrocycle and thread. This suggests that although the strongest intermolecular interactions seem to occur in the *syn-syn* case (closely followed by the *syn-anti* case), there appears to be sufficient intermolecular interactions in each of the three cases to form a stable pseudo-rotaxane. A zero-point energy correction was also considered, and was found to have no significant impact on the size of the binding energies (slightly reducing the values, by less ten percent in each case). The zero-point corrected binding energy for the most stable conformation (*syn-syn*) was found to be around 224 kJ mol^{-1}.
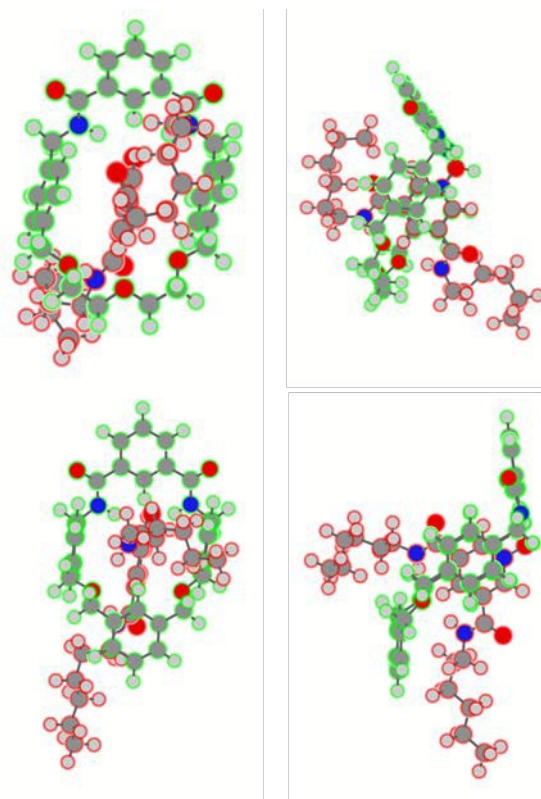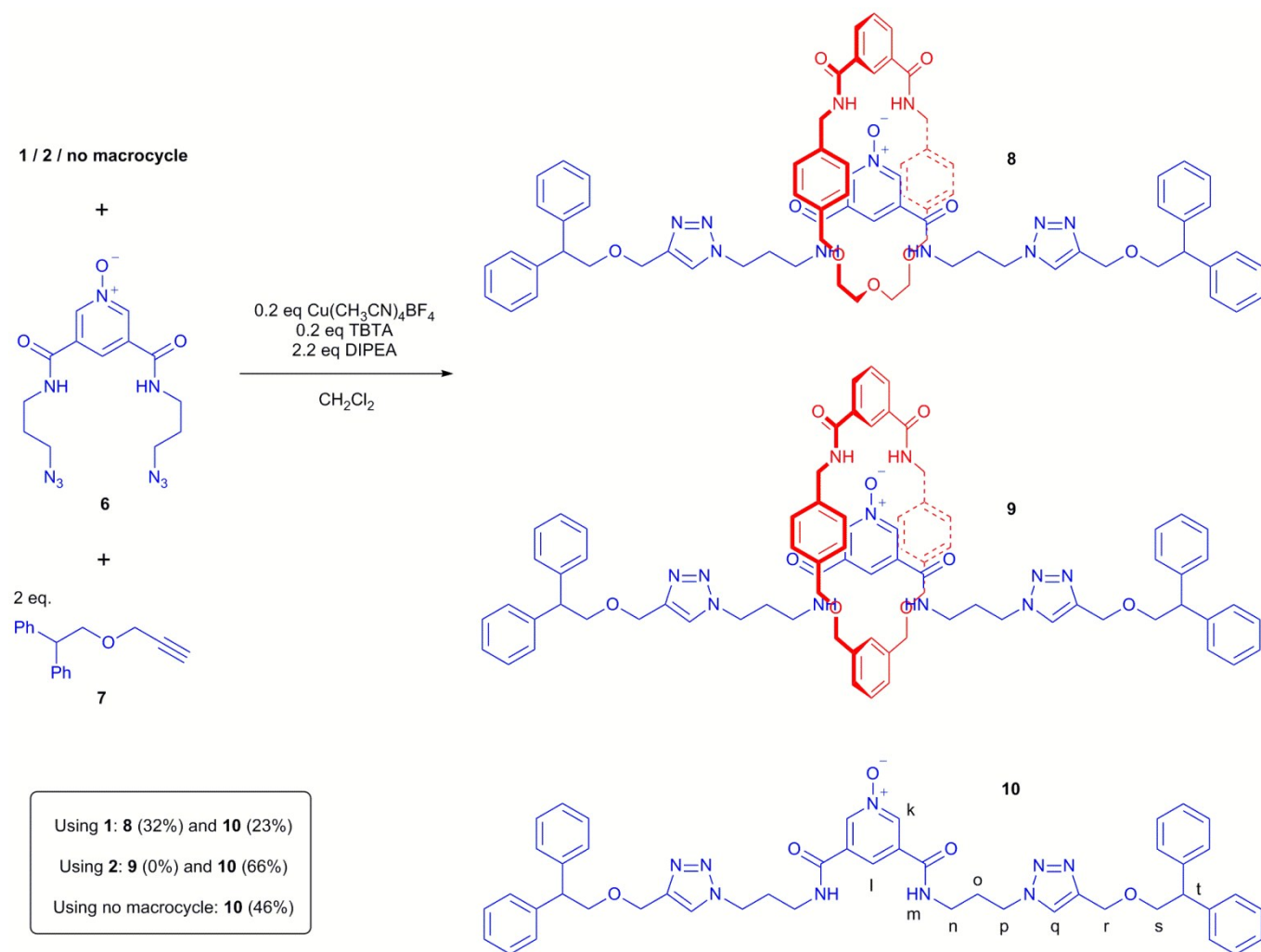

Figure 6: Optimised structures of pseudo-rotaxane **1·5** (top) and **2·5** (bottom) from DFT calculations. Two views of each pseudo-rotaxane are shown to highlight similarities of macrocycle-thread configurations and interactions in the two modelled pseudo-rotaxanes.

In the absence of a crystal structure, only 'free-hand' structures for pseudo-rotaxane **2·5**, drawn to maximise intermolecular interactions as starting points for the geometry optimisations, were considered. The structures used were qualitatively similar to those obtained for pseudo-rotaxane **1·5**. The results of the geometry optimisations were consistent with those of the other pseudo-rotaxane, with the *syn-syn* conformation being the most stable, closely followed by *syn-anti*, with the *anti-anti* conformation being the least stable. As for **1·5**, there is correlation between the O-H$_c$ distance and the stability of the conformation (see Table 1). The average ring-ring distances fall in the range 3.63 – 3.83 Å, which once again are similar to those observed for **1·5**.

Scheme 3: Attempted syntheses of rotaxanes **8** and **9** and non-interlocked axle **10**.

A similar examination of the relative stability of the pseudo-rotaxane **2·5** (with the three distinct thread conformations) was undertaken, quantifying the stability of the pseudo-rotaxane relative to the individual thread and macrocycle, and attempting to quantify the intermolecular interactions in the pseudo-rotaxane. Once again, the *syn-syn* conformation (depicted in Figure 6) was the most stable relative to the individual thread and macrocycle, and the least stable was the *anti-anti* conformation. The relative behaviour of these two conformations was essentially the same as observed for pseudo-rotaxane **1·5**, with the latter being 32 kJ mol^{-1} higher in energy. However, unlike for pseudo-rotaxane **1·5**, the *syn-anti* conformation was similar in energy to the *anti-anti* conformation, rather than the *syn-syn* conformation, being 30 kJ mol^{-1} higher in energy than the *syn-syn*. Importantly, and perhaps counter-intuitively given that pseudo-rotaxane **2·5** is not experimentally observed, a similar binding energy for **2·5** to that of **1·5** was calculated. For **2·5**, the zero-point corrected binding energy for the most stable conformation (*syn-syn*) was found to be around 213 kJ mol^{-1}, only 10 kJ mol^{-1} smaller than in the case of **1·5**.

To explain why pseudo-rotaxane **1·5** forms but **2·5** does not, requires a consideration of the minimized structures of macrocycles **1** and **2** derived from the crystal structures of these two species (which were found to be of lower energy than the minimized structures of **1** and **2** taken from the simulations of pseudo-rotaxanes **1·5** and **2·5**). While the minimized structure of isolated macrocycle **1** is similar to that of the macrocycle in pseudo-rotaxane **1·5**, isolated macrocycle **2** has a remarkably broad cavity – and clearly would require significant rearrangement to achieve the correct geometry to form the hydrogen bonds and π-π stacking of pseudo-rotaxane **2·5**. We therefore propose that a high energy barrier exists that disfavours reorganization of macrocycle **2**, to account for lack of pseudo-rotaxane formation in this case.

Rotaxane synthesis

Following the pseudo-rotaxane studies, attention turned to preparing fully interlocked rotaxanes by use of CuAAC conditions to stopper a bis-azide pyridine-*N*-oxide in the presence of an isophthalamide macrocycle (Scheme 3). The reactions attempted involved dissolving either macrocycle **1** or

2 in dichloromethane under an inert atmosphere, adding 1 equivalent of pyridine-*N*-oxide bis-azide **6**[11] followed by 2 equivalents of alkyne stopper **7**[21]. Then 0.2 equivalents of Cu(CH₃CN)₄BF₄ and TBTA were added, followed by 2.2 equivalents of *N,N*-diisopropylamine. The reactions were stirred overnight at room temperature, and then submitted to an aqueous work-up and purification by silica gel chromatography. Non-interlocked axle **10** was first prepared (by not using either **1** or **2**) to verify these conditions would successfully react the components **6** and **7**.[22]

Using macrocycle **1**, rotaxane **8** was isolated in a 32% yield. In contrast, using macrocycle **2**, unsurprisingly no rotaxane **9** was observed in the crude ¹H NMR spectrum, with only macrocycle **2** and non-interlocked axle **10** being isolated after column chromatography. These results were consistent with the pseudo-rotaxane studies using macrocycles **1** and **2** with pyridine-*N*-oxide thread **5**.

The ¹H NMR spectrum of rotaxane **8**, along with that of non-interlocked macrocycle **1** and axle **10** for comparison, is shown in Figure 7.[23] The downfield shifts of protons *c* and *d* in the rotaxane compared to the non-interlocked macrocycle are indicative of hydrogen bonding to the oxygen atom of the pyridine-*N*-oxide of the axle component. The upfield shift and splitting of protons *f* and *g* are, as for pseudo-rotaxane **1·5**, consistent with intercalation of the pyridine-*N*-oxide ring of the axle between the aromatic rings of the macrocycle.

The interlocked nature of rotaxane **8** was further supported by the appearance of multiple through-space correlations being observed in the ¹H-¹H ROESY NMR spectrum between signals arising from protons in the macrocyclic and axle components (Figure 8). Most clearly, the *ortho*-pyridinium proton *k* of the axle interacts with protons *c*, *f* and *g* (and possibly *d*) of the macrocyclic component. In addition, molecular ion peaks for the rotaxane are readily identifiable at *m/z* 1294.60 and 1316.59 corresponding to the H⁺ and Na⁺ adducts in the positive-ion electrospray MS (see ESI†).[24, 25]

Conclusions

The production in reasonable yield of a fully interlocked rotaxane comprising a 3,5-bisamide pyridine-*N*-oxide axle threaded through an isophthalamide macrocycle relying solely on hydrogen bond template interactions is possible, without recourse to an additional ionic template. However, successful pseudo-rotaxane (and hence rotaxane) formation is dependent on the structure of the macrocycle, as rationalised in this study by a combination of NMR spectroscopy, X-ray crystallography and, importantly, computational modelling.

The general architecture of rotaxane **8** presents numerous opportunities for incorporating functionality by use of appropriate precursors, for example on the axle and/or through the 5 position of the isophthalamide ring. The exploitation of this synthetic methodology, including the development of rotaxanes that can act as receptors for ionic and small molecular guests, is ongoing in our laboratories.
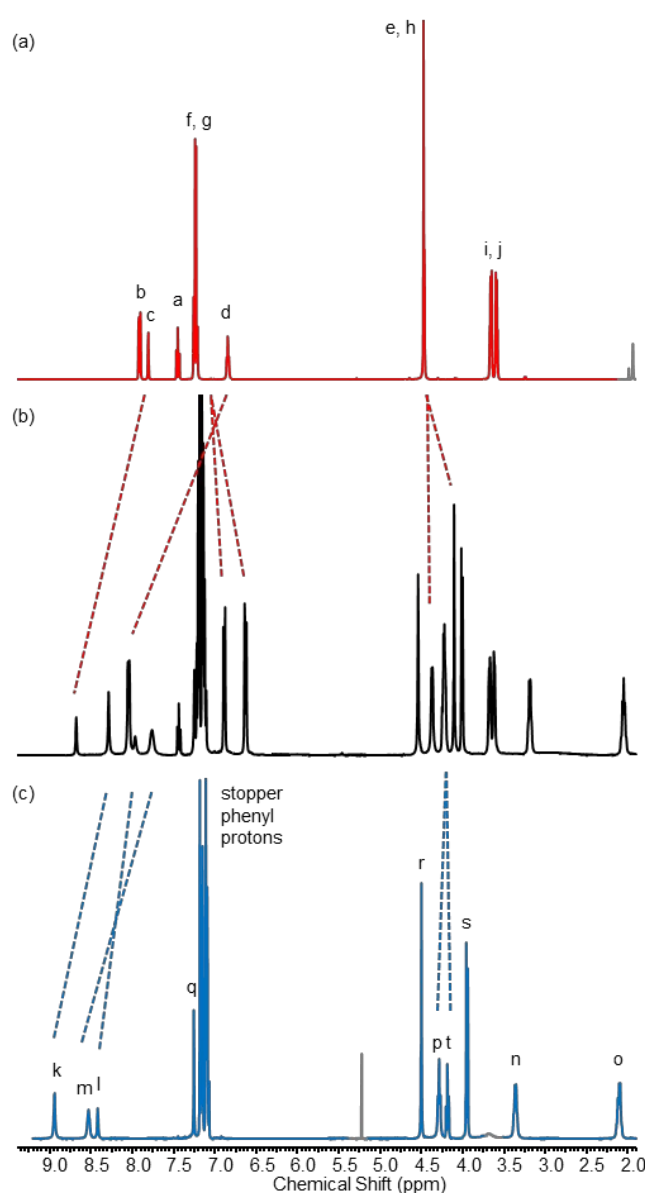

Figure 7: ¹H NMR spectra of (a) macrocycle **1** (b) rotaxane **8** and (c) axle **10** (CDCl₃, 400 MHz, 298 K). For atom labels see Figure 2 and Scheme 3. Trace solvent peaks are coloured grey.

Experimental

General information

Commercially available solvents and chemicals were used without further purification unless stated. Dry solvents, NEt₃ and DIPEA were purchased dry and stored under an inert atmosphere. Cu(CH₃CN)₄BF₄ was stored in a desiccator over P₄O₁₀. Deionised water was used in all cases. Compounds **1**[14] and **6**[11] were prepared as previously reported. Details regarding the preparation of compounds **5** and **7** may be found in the ESI†.

Silica gel with a 60Å particle size was used as the stationary phase for column chromatography. Analytical TLC was used to monitor the progress of column chromatography and
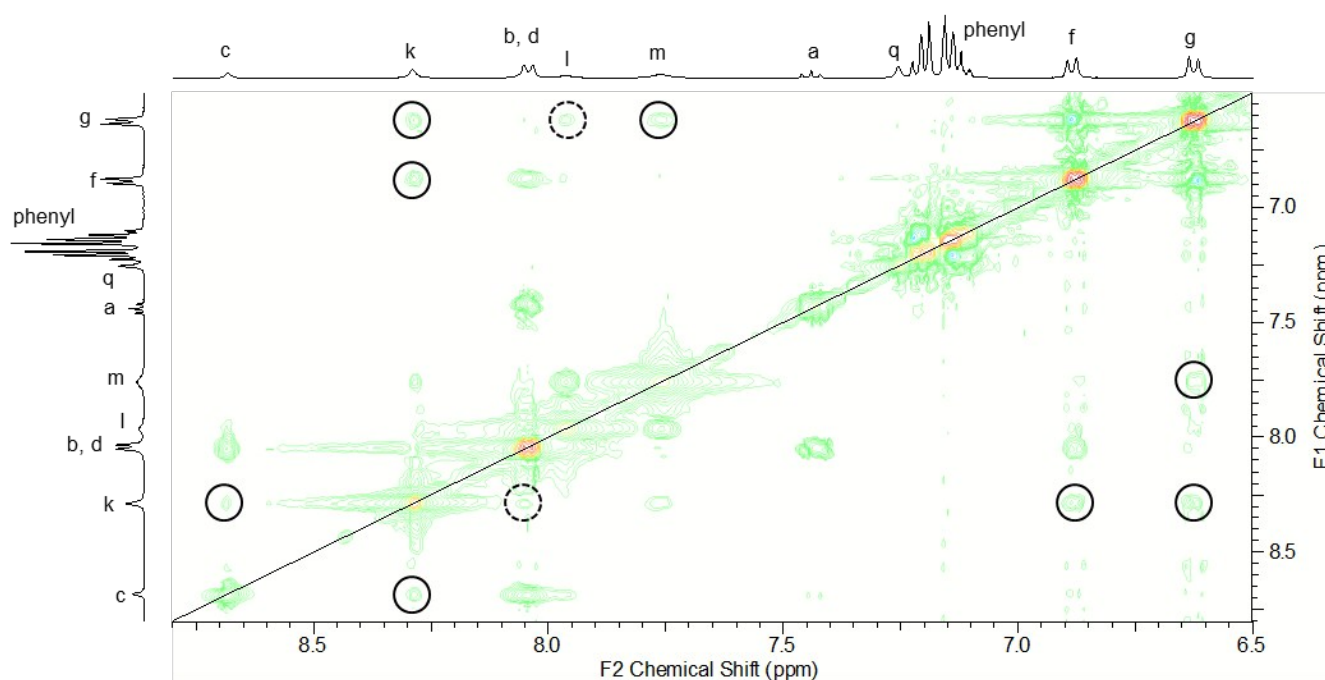
Figure 8: ^{1}H-^{1}H ROESY NMR spectrum of rotaxane **8** (CDCl$_3$, 400 MHz, 298 K). Inter-component through-space cross-peaks are circled. Cross-peaks that appear on only one side of the diagonal are enclosed by a dashed circle.

analytical TLC plates were typically examined under short wavelength (λ = 254 nm) UV light. If required, ceric ammonium molybdate or potassium permanganate stains were used to develop the analytical TLC plates.

IR spectra were recorded on an Agilent Technologies Cary 630 FTIR spectrometer. NMR spectra were recorded on a Bruker Ultrashield 400 Plus spectrometer at 298 K, with the NMR data for **8** and **10** reported below assigned according to the atom labels to be found in Figure 2 and Scheme 3. Mass spectra were recorded on a Thermofisher LTQ Orbitrap XL at the EPSRC UK National Mass Spectrometry Facility at Swansea University, UK, or a Shimadzu LCMS IT ToF instrument at Lancaster University, UK. Melting points were recorded on a Gallenkamp capillary melting point apparatus and are uncorrected.

Experimental procedures

Macrocycle **2**. Isophthaloyl chloride (162 mg, 0.797 mmol) dissolved in CH$_2$Cl$_2$ (150 mL) and bis-amine **4** (300 mg, 0.797 mmol) dissolved in CH$_2$Cl$_2$ (150 mL) containing 0.6 mL NEt$_3$ (to aid dissolution of **4**) was added dropwise to a solution of NEt$_3$ (0.4 mL) in CH$_2$Cl$_2$ (200 mL). The reaction was stirred under an Ar (g) atmosphere for 16 h. The reaction mixture was concentrated to 100 mL, then washed with 1 M HCl (aq) (1 × 100 mL) and 1 M KOH (aq) (1 × 100 mL). The organic layer was separated, dried (MgSO$_4$), filtered and concentrated to give a white solid. The crude material was purified by silica gel column chromatography (99 : 1 CH$_2$Cl$_2$/CH$_3$OH to yield the title compound, with (as identified by ^{1}H NMR spectroscopy) one equivalent of CH$_2$Cl$_2$, as a white solid (177 mg, 38%). R_f = 0.27, 98 : 2 CH$_2$Cl$_2$/CH$_3$OH. Mp multiple phase transitions between

208–220 °C. υ_{max}/cm^{-1} (neat) 3330 (N–H), 2940 (C–H), 2860 (C–H), 2830 (C–H), 1640 (C=O), 1530 (N–H), 1070 (C–O). δH(400 MHz; CDCl$_3$) 7.94 (2H, d, ^3J = 7.7 Hz, isophthalamide H^4 & H^6), 7.81 (1H, s, isophthalamide H^2), 7.48 (1H, t, ^3J = 7.7 Hz, isophthalamide H^5), 7.29–7.38 (12H, m, aromatic H), 6.74 (2H, br s, NH), 4.50–4.55 (12H, m, 3 × CH_2). δC(100 MHz; CDCl$_3$) 166.9 (C=O), 138.4, 137.7, 137.2, 134.6, 130.9, 129.5, 128.5, 128.4, 128.2, 126.9, 126.6, 123.8 (12 Ar C environments), 71.9, 71.7 (2 × OCH$_2$), 44.0 (NHCH$_2$). m/z (ES) 541.1900 ([M + Cl]$^-$, C$_{32}$ClH$_{30}$N$_2$O$_4$ requires 541.1900).

Bis-nitrile **3**. NaH (60% dispersion in mineral oil, 300 mg, 7.51 mmol) was added to a solution of (benzene-1,3-diyl)dimethanol (400 mg, 2.90 mmol) in dry THF (25 mL) under an Ar (g) atmosphere. Then 4-(bromomethyl)benzonitrile (1.19 g, 6.08 mmol) was added and the reaction heated under reflux for 16 h under an Ar (g) atmosphere. After careful quenching with H$_2$O, the reaction mixture was extracted with EtOAc (3 × 20 mL). The combined organic layers were dried (MgSO$_4$), filtered and concentrated to give a viscous yellow oil. This material was taken up EtOAc and petrol 40-60 added causing precipitation of the title compound. This was isolated by vacuum filtration as an off-white solid (798 mg, 73%). Mp 78–80 °C. υ_{max}/cm^{-1} (neat) 3080 (C–H), 2930 (C–H), 2850 (C–H), 2220 (nitrile C–N), 1610 (ring C=C), 1110 (C–O). δH(400 MHz; CDCl$_3$) 7.64 (4H, d, ^3J = 8.2 Hz, aromatic H), 7.47 (4H, d, ^3J = 8.2 Hz, aromatic H), 7.31-7.40 (4H, m, aromatic H), 4.62 (4H, s, CH_2), 4.60 (4H, s, CH_2). δC(100 MHz; CDCl$_3$) 143.7, 138.0, 132.2, 128.7, 127.7, 127.3, 127.0, 118.8, 111.3 (6 Ar C & the nitrile CN environments), 72.6, 71.2 (2 × CH$_2$). m/z (ES) 386.1865 ([M + NH$_4$]$^+$, C$_{24}$H$_{24}$N$_3$O$_2$ requires 386.1863).

Bis-amine **4**. 1 M BH$_3$·THF (6 mL) was carefully added to a solution of bis-nitrile **3** (300 mg, 0.814 mmol) in dry THF (6 mL)

ARTICLE

under an Ar (g) atmosphere. The reaction was heated under reflux for 8 h and then stirred at RT for 16 h, under an Ar (g) atmosphere. CH_3OH was added carefully to quench the reaction, then 2 mL of conc. HCl (aq) added, producing a white precipitate. After stirring for 10 minutes, the reaction mixture was co-evaporated with CH_3OH. The resulting material was suspended in CH_2Cl_2 (25 mL) and stirred with 10% NaOH (aq) (25 mL) for 30 min. The organic layer was separated, washed with H_2O (1 × 25 mL), dried ($MgSO_4$), filtered and solvent removed *in vacuo* to give the title compound as a white solid (149 mg, 40%). Mp 100–104 °C. υ_{max}/cm^{-1} (neat) 2840-3350 (broad N–H & multiple C–H). δH(400 MHz; $CDCl_3$) 7.29–7.37 (12H, m, aromatic *H*), 4.55 (8H, s, 2 × OC*H*$_2$), 3.87 (4H, s, NC*H*$_2$). δC(100 MHz; $CDCl_3$) 142.8, 138.5, 136.7, 128.5, 128.1, 127.1, 127.1 (sic), 127.0 (8 Ar C environments), 71.9 (2 OCH_2 – coincident), 46.3 (NH_2CH_2). *m/z* (ES) 377.2225 ([M + H]$^+$, $C_{24}H_{29}N_2O_2$ requires 377.2224).

Rotaxane **8**. Macrocycle **1** (25 mg, 0.053 mmol) and pyridine-*N*-oxide bis-azide **6** (18 mg, 0.053 mmol) were dissolved in dry CH_2Cl_2 (5 mL) under an Ar (g) atmosphere. Then alkyne stopper **7** (25 mg, 0.11 mmol), $Cu(CH_3CN)_4BF_4$ (3.3 mg, 0.011 mmol), TBTA (5.6 mg, 0.011 mmol) and DIPEA (20 µL, 15 mg, 0.12 mmol) were added. The reaction was stirred at RT for 18 h under an Ar (g) atmosphere. Then, the reaction was dilute to 20 mL, washed with 0.02 M EDTA in 1 M NH_3 (aq) solution (2 × 10 mL) and (1 × 10 mL) brine. The organic layer was dried ($MgSO_4$), filtered and solvent removed *in vacuo*. The crude material was purified by silica gel column chromatography (98:2 to 92:8 CH_2Cl_2/CH_3OH) to give the title compound as a foaming white solid (22 mg, 32%). R_f = 0.14, 98 : 2 CH_2Cl_2/CH_3OH. Mp 150 °C (dec). υ_{max}/cm^{-1} (neat) 3350 (N–H), 3060 (C–H), 2860 (C–H), 1650 (C=O), 1540 (N–O). δH(400 MHz; $CDCl_3$) 8.68 (1H, s, *H*^{c}), 8.29 (2H, s, *H*^{k}), 8.04–8.05 (5H, m, *H*^{b} & *H*^{d}), 7.96 (1H, s, *H*^{l}), 7.76 (2H, s, *H*^{m}), 7.44 (1H, t, ^3J = 7.8 Hz, *H*^{a}), 7.10–7.25 (22H, m, aromatic *H* & *H*^{q}), 6.89 (4H, d, ^3J = 7.8 Hz, *H*^{f}), 6.62 (4H, d, ^3J = 7.8 Hz, *H*^{g}), 4.54 (4H, s, *H*^{r}), 4.37 (4H, s, *H*^{e}), 4.20–4.24 (6H, m, *H*^{p} & *H*^{t}), 4.10 (4H, s, *H*^{h}), 4.00 (4H, d, ^3J = 7.2 Hz, *H*^{s}), 3.63–3.68 (8H, m, *H*^{i} & *H*^{j}), 3.18–3.20 (4H, m, *H*^{n}), 2.04–2.07 (4H, m, *H*^{o}). δC(100 MHz; $CDCl_3$) 166.8, 162.5 (2 × C=O), 145.0, 141.9, 140.0, 138.3, 135.4, 134.0, 132.3, 131.3, 129.1, 128.5, 128.4, 128.2, 126.5, 126.0, 124.9, 123.1 (17 pyridyl, aromatic & triazole C environments – including a coincident pair), 73.8, 70.9, 69.9, 64.4, 51.0, 47.8, 43.9, 37.2, 30.0 (10 × sp^3 C – including a coincident pair). *m/z* (ES) 1294.6091 ([M + H]$^+$, $C_{75}H_{80}N_{11}O_{10}$ requires 1294.6084); 1316.5940 ([M + Na]$^+$, $C_{75}H_{79}N_{11}NaO_{10}$ requires 1316.5904).

Rotaxane **9**. An analogous reaction to that for rotaxane **8** was carried out, substituting macrocycle **2** for macrocycle **1** in the reaction mixture. After the aqueous workup, no rotaxane **9** was identifiable in the ^{1}H NMR spectrum of the crude reaction mixture, and after column chromatography only macrocycle **2** and axle **10** were recovered.

Axle **10**. An analogous reaction to that for rotaxane **8** was carried out, omitting macrocycle **1** from the reaction mixture. After the aqueous workup, the crude material was purified by silica gel chromatography (96 : 4 to 92 : 8 CH_2Cl_2/CH_3OH) to give the title compound as a transparent colourless glass

(22 mg, 47%). R_f = 0.17, 96 : 4 CH_2Cl_2/CH_3OH. υ_{max}/cm^{-1} (neat) 3270 (N–H), 3060 (C–H), 2860 (C–H), 1670 (C=O), 1540 (N–O). δH(400 MHz; $CDCl_3$) 8.94 (2H, s, *H*^{k}), 8.54 (2H, br s, *H*^{m}), 8.42 (1H, s, *H*^{l}), 7.26 (2H, s, *H*^{q}), 7.07–7.18 (20H, m, aromatic *H*), 4.50 (4H, s, *H*^{r}), 4.28 (4H, t, ^3J = 6.4 Hz, *H*^{p}), 4.18 (4H, t, ^3J = 7.3 Hz, *H*^{t}), 3.94 (4H, d, ^3J = 7.3 Hz, *H*^{s}), 3.35–3.37 (4H, m, *H*^{n}), 2.10–2.13 (4H, m, *H*^{o}). δC(100 MHz; $CDCl_3$) 162.2 (C=O), 145.1, 141.9, 140.3, 133.7, 128.4, 128.2, 126.5, 123.2 (9 pyridyl, aromatic & triazole C environments – including a coincident pair), 73.8, 64.3, 50.9, 48.2, 37.5, 29.3 (6 × sp^3 C). *m/z* (ES) 820.3939 ([M + H]$^+$, $C_{47}H_{50}N_9O_5$ requires 820.3939).

Computational methodology

All calculations were performed using Gaussian 09 version E01;[18] structures were visualised with Gaussview 5.09. Density-functional theory was employed to study the electronic and molecular structure of all of the systems, using the conventional Kohn–Sham approach. The B3LYP[19] exchange–correlation functional was used (as defined in Gaussian 09, with VWN3 in the correlation functional definition, rather than the conventional VWN5 definition[25]), alongside the 6-31G* all-electron basis set on all atoms. The general use of larger basis sets was prohibitively expensive due to the size of the molecules (at least for the optimisations), and where tested did not change any of the conclusions. The default integration grid was employed for all calculations.

For all calculations, solvent effects were modelled using the polarisable continuum model (PCM); the default Gaussian 09 cavity parameters were used based on the UFF radii, with chloroform as the continuum solvent.

Dispersion effects were approximated using the D3 approach of Grimme,[20] with the parameters as recommended for the B3LYP functional.

Frequency calculations were undertaken to ensure that the stationary points found were in fact minima on the potential energy surfaces, and also to allow for zero-point energy corrections to the energetic data.
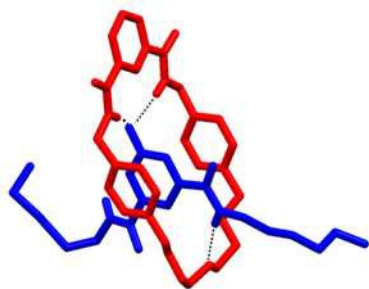
Acknowledgements

All underlying data for this paper are provided in the experimental section and the ESI. Electronic copies of NMR
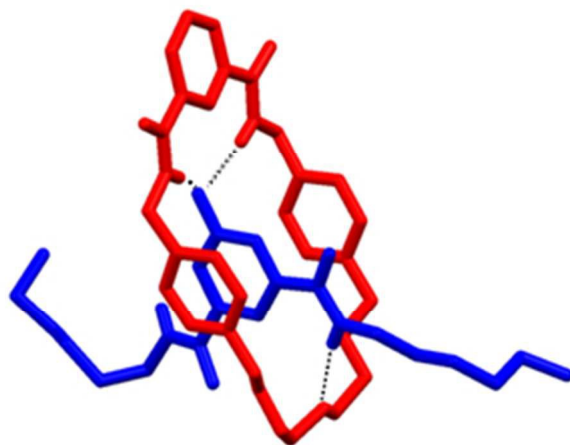
spectra (including fid files) are available from DOI: 10.17635/lancaster/researchdata/90.

Notes and references

1   M. Xue, Y. Yang, X. Chi, X. Yan and F. Huang, *Chem. Rev.*, 2015, **115**, 7398-7501.
2   For a review on functional rotaxanes, see: S. F. M. van Dongen, S. Cantekin, J. A. A. W. Elemans, A. E. Rowan and R. J. M. Nolte, *Chem. Soc. Rev.*, 2014, **43**, 99-122.
3   For some very recent examples of functional rotaxanes, see: (a) R. Barat, T. Legigan, I. Tranoy-Opalinski, B. Renoux, E. Péraudeau, J. Clarhaut, P. Poinot, A. E. Fernandes, V. Aucagne, D. A. Leigh and S. Papot, *Chem. Sci.*, 2015, **6**, 2608-2613; (b) M. Galli, J. E. M. Lewis and S. M. Goldup, *Angew. Chem. Int. Ed.*, 2015, **54**, 13545-13549; (c) S. Guha, G. K. Shaw, T. M. Mitcham, R. R. Bouchard and B. D. Smith, *Chem. Comm.*, 2016, **52**, 120-123; (d) Y. Cakmak, S. Erbas-Cakmak and D. A. Leigh, *J. Am. Chem. Soc.*, 2016, **138**, 1749-1751; (e) G. Yu, D. Wu, Y. Li, Z. Zhang, L. Shao, J. Zhou, Q. Hu, G. Tang and F. Huang, *Chem. Sci.*, 2016, **7**, 3017-3024.
4   (a) C. Wu, P. R. Lecavalier, Y. X. Shen and H. W. Gibson, *Chem. Mater.*, 1991, **3**, 569; (b) J.-C. Chambron, V. Heitz and J.-P. Sauvage, *J. Chem. Soc., Chem. Commun.*, 1992, 1131-1133; (c) L. Hogg, D. A. Leigh, P. J. Lusby, A. Morelli, S. Parsons and J. K. Y. Wong, *Angew. Chem. Int. Ed.*, 2004, **43**, 1218-1221; (d) A. M. Fuller, D. A. Leigh, P. J. Lusby, I. D. H. Oswald, S. Parsons, D. B. Walker, *Angew. Chem. Int. Ed.*, 2004, **43**, 3914-3918; (e) S. M. Goldup, D. A. Leigh, P. J. Lusby, R. T. McBurney and A. M. Z. Slawin, *Angew. Chem. Int. Ed.*, 2008, **47**, 6999-7003; (f) V. Aucagne, K. D. Hanni, D. A. Leigh, P. J. Lusby and D. B. Walker, *J. Am. Chem. Soc.*, 2006, **128**, 2186-2187; (g) H. Lahlali, K. Jobe, M. Watkinson and S. M. Goldup, *Angew. Chem. Int. Ed.*, 2011, **50**, 4151-4155; (h) A. Noor, S. C. Moratti and J. D. Crowley, *Chem. Sci.*, 2014, **5**, 4283-4290.
5   (a) G. M. Hübner, J. Gläser, C. Seel and F. Vögtle, *Angew. Chem. Int. Ed.*, 1999, **38**, 383-386; (b) C. A. Schalley, G. Silva, C. F. Nising, P. Linnartz, *Helv. Chim. Acta*, 2002, **85**, 1578-1596; (c) J. A. Wisner, P. D. Beer, M. G. B. Drew and M. R. Sambrook, *J. Am. Chem. Soc.*, 2002, **124**, 12469-12476; (d) E. Arunkumar, C. C. Forbes, B. C. Noll and B. D. Smith, *J. Am. Chem. Soc.*, 2005, **127**, 3288-3289; (e) L. M. Hancock and P. D. Beer, *Chem. Eur. J.*, 2009, **15**, 42-44; (f) M. J. Langton, L. C. Duckworth and P. D. Beer, *Chem. Commun.*, 2013, **49**, 8608-8610.
6   (a) P. R. Ashton, M. Grognuz, A. M. Z. Slawin, J. F. Stoddart and D. J. Williams, *Tetrahedron Lett.*, 1991, **32**, 6235-6238; (b) R. A. Bissell, E. Córdova, A. E. Kaifer and J. F. Stoddart, *Nature*, 1994, **369**, 133-137; (c) M. J. Gunter, N. Bampos, K. D. Johnstone and J. K. M. Sanders, *New J. Chem.*, 2001, **25**, 166-173.
7   (a) F. G. Gatti, D. A. Leigh, S. A. Nepogodiev, A. M. Z. Slawin, S. J. Teat and J. K. Wong, *J. Am. Chem. Soc.*, 2001, **123**, 5983-5989; (b) D. M. D'Souza, D. A. Leigh, L. Mottier, K. M. Mullen, F. Paolucci, S. J. Teat and S. Zhang, *J. Am. Chem. Soc.*, 2010, **132**, 9465-9470; (c) A. Altieri, V. Aucagne, R. Carrillo, G. J. Clarkson, D. M. D'Souza, J. A. Dunnett, D. A. Leigh and K. M. Mullen, *Chem. Sci.*, 2011, **2**, 1922-1928; (d) R. Ahmed, A. Altieri, D. M. D'Souza, D. A. Leigh, K. M. Mullen, M. Papmeyer, A. M. Z. Slawin, J. K. Y. Wong and J. D. Woollins, *J. Am. Chem. Soc.*, 2011, **133**, 12304-12310; (e) A. Tron, P. J. Thornton, M. Rocher, H.-P. J. de Rouville, J.-P. Desvergne, B. Kauffmann, T. Buffeteau, D. Cavagnat, J. H. R. Tucker and N. D. McClenaghan, *Org. Lett.*, 2014, **16**, 1358-1361.
8   M. Chen, S. Han, L. Jiang, S. Zhou, F. Jiang, Z. Xu, J. Liang and S. Zhang, *Chem. Commun.*, 2010, **46**, 3932-3934.

9   Additional Na⁺ or Ba²⁺ template: L. M. Hancock and P. D. Beer, *Chem Commun.*, 2011, **47**, 6012-6014. Yields: (Na⁺) 50%, (Ba²⁺) 28%; (no cation) 10%.
10 Additional Na⁺ template: R. C. Knighton and P. D. Beer, *Chem. Commun.*, 2014, **50**, 1540-1542. Yield: (Na⁺) 62%; (no cation) < 10%.
11 Additional Ln³⁺ template: F. Zapata, O. A. Blackburn, M. J. Langton, S. Faulkner and P. D. Beer, *Chem. Commun.*, 2013, **49**, 8157-8159. Yield: (Ln³⁺) 20%. In this system it was not possible to determine the yield in the absence of a cationic template, as the macrocycle would sequester the Cu cation being used in the CuAAC reaction being used to stopper the rotaxane.
12 Additional Cl⁻ template: J. M. Mercurio, F. Tyrrell, J. Cookson and P. D. Beer, *Chem. Commun.*, 2013, **49**, 10793-10795. Yields: (Cl⁻) 9%-17%; (no Cl⁻) 0%.
13 L. M. Hancock, DPhil Thesis, University of Oxford, 2011.
14 C. N. Marrs and N. H. Evans, *Org. Biomol. Chem.*, 2015, **13**, 11021-11025.
15 See ESI for synthetic details about thread **5**.
16 Due to peak broadening it is hard to assign with confidence peaks *c* and *d* in the ¹H NMR of pseudo-rotaxane **1·3**. It is expected that these peaks will have moved downfield due to hydrogen bonding to the oxygen of the pyridine-*N*-oxide.
17 See ESI for further images from the computational simulations and for coordinate data files.
18 Gaussian 09, Revision E.01, M. J. Frisch, G. W. Trucks, H. B. Schlegel, G. E. Scuseria, M. A. Robb, J. R. Cheeseman, G. Scalmani, V. Barone, B. Mennucci, G. A. Petersson, H. Nakatsuji, M. Caricato, X. Li, H. P. Hratchian, A. F. Izmaylov, J. Bloino, G. Zheng, J. L. Sonnenberg, M. Hada, M. Ehara, K. Toyota, R. Fukuda, J. Hasegawa, M. Ishida, T. Nakajima, Y. Honda, O. Kitao, H. Nakai, T. Vreven, J. A. Montgomery, Jr., J. E. Peralta, F. Ogliaro, M. Bearpark, J. J. Heyd, E. Brothers, K. N. Kudin, V. N. Staroverov, R. Kobayashi, J. Normand, K. Raghavachari, A. Rendell, J. C. Burant, S. S. Iyengar, J. Tomasi, M. Cossi, N. Rega, J. M. Millam, M. Klene, J. E. Knox, J. B. Cross, V. Bakken, C. Adamo, J. Jaramillo, R. Gomperts, R. E. Stratmann, O. Yazyev, A. J. Austin, R. Cammi, C. Pomelli, J. W. Ochterski, R. L. Martin, K. Morokuma, V. G. Zakrzewski, G. A. Voth, P. Salvador, J. J. Dannenberg, S. Dapprich, A. D. Daniels, Ö. Farkas, J. B. Foresman, J. V. Ortiz, J. Cioslowski, and D. J. Fox, Gaussian, Inc., Wallingford CT, 2009.
19 (a) A. D. Becke, *J. Chem. Phys.*, 1993, **98**, 5648-5652; (b) P. J. Stephens, F. J. Devlin, C. F. Chabalowski, and M. J. Frisch, *J. Phys. Chem.*, 1994, **98**, 11623-11627; (c) A. D. Becke, *J. Chem. Phys.*, 1993, **98**, 1372-1377; (d) C. Lee, W. Yang, and R. G. Parr, *Phys. Rev. B*, 1998, **37**, 785-789.
20 S. Grimme, J. Antony, S. Ehrlich and H. Krieg, *J. Chem. Phys.*, 2010, **132**, 154104.
21 See ESI for synthetic details about stopper **7**.
22 After work-up, analysis of the crude ¹H NMR spectrum suggested a high conversion of **6** and **7** to axle **10**, but after chromatographic purification, **10** was isolated in only a 46% yield. This is attributed to the polar nature of **10** meaning that material was lost on the polar silica stationary phase. Note that **10** was isolated in a 66% yield after column chromatography of the crude reaction mixture from the attempted synthesis of rotaxane **9**.
23 See ESI for ¹³C NMR, IR and high resolution mass spectra of rotaxane **8**.
24 No peaks attributable to either macrocycle **1** or axle **10** were observed in the electrospray MS of rotaxane **8**.
25 S. H. Vosko, L. Wilk, and M. Nusair, Can. J. Phys., 1980, **58**, 1200-1211.

Graphical Abstract

A pyridine-*N*-oxide containing rotaxane, not requiring an additional ionic template, has been prepared in 32% yield. The role of macrocycle structure in successful pseudo-rotaxane formation has been rationalised by a combination of NMR spectroscopy, X-ray crystallography and computational modelling.

50x39mm (150 x 150 DPI)